DOI: 10.1002/zaac.201200277

Preparation, Crystal Structure, Electronic Structure, Impedance Spectroscopy, and Raman Spectroscopy of Li_3SbS_3 and Li_3AsS_3

Sebastian Huber,[a] Christian Preitschaft,[a] Richard Weihrich,[a] and Arno Pfitzner*[a]

Keywords: Thiometalate; Lithium; Crystal structure; Electronic structure; Ion conductor

Abstract. Li_3SbS_3 was synthesized by solid-state reaction of stoichiometric amounts of Li_2S and Sb_2S_3 in the ratio 3:1. The product is air and moisture sensitive. The crystal structure was determined from single crystals at room temperature. Pale grey Li_3SbS_3 crystallizes in the orthorhombic space group $Pna2_1$ (no. 33) with a = 7.9671(5) Å, b = 6.7883(5) Å, c = 10.0912(8) Å, V = 545.76(7) Å^3, and Z = 4 (data at 20 °C). Antimony and sulfur atoms build isolated, trigonal pyramidal $[SbS_3]^{3-}$ units, which are stacked along [100]. These $[SbS_3]^{3-}$ units are connected by $[LiS_x]$-polyhedra. The lithium ions have either a distorted tetrahedral coordination by sulfur in the case of Li2 and Li3 or a distorted square pyramidal environment in the case of Li1. The crystal structure is isotypic with Li_3AsS_3, which was obtained by reaction of stoichiometric amounts of lithium, arsenic, and sulfur in the ratio 3:1:3 in an excess of LiI. LiI serves only as a flux and is not incorporated in the crystal structure. Li_3AsS_3 crystallizes as colorless rods, space group $Pna2_1$ (no. 33) with a = 8.090(1) Å, b = 6.658(1) Å, c = 9.868(1) Å, V = 531.5(1) Å^3, and Z = 4 (data at 20 °C). Both compounds are confirmed as semiconductors with bandgaps close to 3 eV from DFT-calculations with GGA and hybrid functionals. Impedance spectroscopic measurements of Li_3SbS_3 show a specific conductivity of $\sigma = 1.6 \times 10^{-9}$ Ω^{-1} cm^{-1} at 323 K and of $\sigma = 5.4 \times 10^{-5}$ Ω^{-1} cm^{-1} at 573 K. The activation energy is E_A = 0.72 eV. Raman spectra of Li_3SbS_3 are dominated by the stretching modes of the $[SbS_3]^{3-}$ units at 333, 317, and 301 cm^{-1} at room temperature.

Introduction

Chalcogenides and chalcogenometalates are an important class of solids. There is a huge variety of compounds with the general composition $M^I{}_3PnQ_3$ (M = Li, Na, K, Rb, Cs, Cu, Ag; Pn = P, As, Sb, Bi; Q = S, Se, Te) and some of them show a high ionic conductivity. Therefore, these materials become more and more important for the investigation of new solid electrolytes. Compounds like Na_3SbS_3,[1] K_3SbS_3,[1] K_3SbSe_3,[2] Rb_3SbSe_3,[2] Cs_3SbSe_3,[2] Li_3AsS_3,[3,4] Na_3AsS_3,[1,5] Na_3AsSe_3,[6] K_3AsS_3,[1] K_3AsSe_3,[6] K_3BiSe_3, Rb_3BiSe_3, and Cs_3BiSe_3[7,8] have been synthesized and characterized. They all have isolated $[PnQ_3]^{3-}$ units in common. In addition also modifications with a substitution of the alkali metal are well known. Similar compounds containing coinage metals instead of alkali metals are known, i.e., Ag_3AsS_3,[9,10] Ag_3AsSe_3,[11–13] and Ag_3SbS_3,[9] and Cu_3SbS_3,[14–17] and Cu_3SbSe_3.[18] Especially the copper containing thiometalates are currently discussed as thermoelectric materials.[19,20] Isolated thioantimonate units are also observed in mixed chalcogenometalate halides like $(CuI)_2Cu_3SbS_3$,[21,22] $(AgI)_2$-Ag_3SbS_3,[23,24] and $(LiI)_2Li_3SbS_3$,[25] which show a pronounced ionic conductivity in case of the copper and the silver compound. Halide free Li_3SbS_3 is obviously missing in this series of potentially ion conducting compounds. In addition, the question arises whether the green color of Li_3AsS_3 as described in the literature[3] is intrinsic.

Herein we report on the synthesis, the structural characterization, and physical properties of Li_3SbS_3 and a new synthesis route for colorless Li_3AsS_3.[4]

* Prof. Dr. A. Pfitzner
Fax: +49-941-943-814551
E-Mail: arno.pfitzner@chemie.uni-regensburg.de
[a] Institut für Anorganische Chemie
Universität Regensburg
Universitätsstraße 31
93040 Regensburg, Germany

Results and Discussion

Structure Determination

The crystal structures of Li_3SbS_3 and of Li_3AsS_3 were determined by single-crystal X-ray diffraction. Crystallographic data are summarized in Table 1. Atomic coordinates and isotropic displacement parameters are collected in Table 2. Table 3 lists the anisotropic displacement parameters, and Table 4 shows selected interatomic distances and angles.

Structure Description and Discussion

Li_3SbS_3 and Li_3AsS_3 are isotypic and crystallize in the noncentrosymmetric orthorhombic space group $Pna2_1$. The basis of this structure type are isolated, trigonal pyramidal (ψ-tetrahedral) $[PnS_3]^{3-}$ units. These units are stacked in a kind of zigzag manner along a (see Figure 1). The distances d(Sb–S) in the $[SbS_3]^{3-}$ units are about 2.43 Å, and for d(As–S) about 2.26 Å are observed. In both compounds no additional sulfur atoms are found in the range of 3.7 Å. The trigonal PnS_3 pyramids are interconnected by $[LiS_x]$ polyhedra. Herein Li2 and Li3 have a distorted tetrahedral environment $[LiS_4]$ with d(Li2–S) = 2.41(1)–2.49(1) Å and d(Li3–S) = 2.42(1)–

Table 1. Crystallographic data for the structure analysis of Li_3SbS_3 and Li_3AsS_3.

	Li_3SbS_3	Li_3AsS_3
Formula weight /g·mol^{-1}	238.75	191.92
Color	pale grey	colorless
Crystal system	orthorhombic	orthorhombic
Space group	$Pna2_1$ (No. 33)	$Pna2_1$ (No. 33)
Lattice constants	a = 7.9671(5) Å	a = 8.090(1) Å
from single crystal data	b = 6.7883(5) Å	b = 6.658(1) Å
	c = 10.0912(8) Å	c = 9.868(1) Å
Cell volume, Z	545.76(7) Å^3, 4	531.5(1) Å^3, 4
ρ_{calc} /g·cm^{-3}	2.906	2.398
Diffractometer	Oxford Diffraction Gemini R Ultra CCD, Mo-K_α, λ = 0.71073 Å	STOE IPDS, Mo-K_α, λ = 0.71073 Å, oriented graphite monochromator
Absorption correction	Multi-scan [29]	Numerical, crystal description with 12 faces, shape optimized with X-SHAPE [31]
Temperature /°C	20	20
2Θ-range /°	$7.2 \le 2\Theta \le 56.7$	$7.9 \le 2\Theta \le 58.1$
hkl range	$-10 \le h \le 10$	$-11 \le h \le 11$
	$-8 \le k \le 9$	$-8 \le k \le 8$
	$-12 \le l \le 11$	$-13 \le l \le 13$
No. of reflections, R_{int}	3126, 0.0356	7095, 0.0265
No. of independent reflections	1109	1354
No. of parameters	63	64
Program	SHELX 97[30]	SHELX 97[30]
Final R/wR ($I > 2\sigma_i$)	0.0251, 0.0484	0.0130, 0.0304
Final R/wR (all reflections)	0.0337, 0.0512	0.0136, 0.0306
GooF	1.036	1.043
Largest difference peak Δp_{max}	0.754	0.311
and hole Δp_{min} /e·Å^{-3}	–0.633	–0.307
Extinction coefficient	–	0.020(1)
Flack parameter	–0.07(8)	0.002(6)

Table 2. Atomic coordinates and equivalent isotropic displacement parameters U_{eq} for Li_3SbS_3 and Li_3AsS_3. All atoms are located on the Wyckoff position 4*a*.

Li_3SbS_3				
Atom	x	y	z	U_{eq} [a]
Sb	0.7354(1)	0.8951(1)	0	0.016(1)
S1	0.8373(4)	0.6965(5)	0.8174(4)	0.018(1)
S2	0.9633(2)	0.1362(2)	0.0083(5)	0.018(1)
S3	0.8207(4)	0.7040(5)	0.1927(4)	0.019(1)
Li1	0.054(2)	0.960(2)	0.776(2)	0.038(3)
Li2	0.912(1)	0.343(2)	0.818(1)	0.023(3)
Li3	0.761(2)	0.375(2)	0.114(1)	0.032(3)
Li_3AsS_3				
Atom	x	y	z	U_{eq} [a]
As	0.2467(1)	0.0972(1)	0	0.015(1)
S1	0.1607(1)	0.2909(1)	0.1733(1)	0.018(1)
S2	0.0445(1)	0.8601(1)	0.9902(1)	0.017(1)
S3	0.1847(1)	0.2803(1)	0.8139(1)	0.018(1)
Li1	0.9343(4)	0.0495(6)	0.2184(4)	0.031(1)
Li2	0.0784(4)	0.6462(5)	0.1889(3)	0.026(1)
Li3	0.2513(4)	0.6156(6)	0.8890(4)	0.029(1)

a) U_{eq} is defined as one third of the trace of the orthogonalized U_{ij} tensor.

2.60(1) Å in Li_3SbS_3, and d(Li2–S) = 2.439(3)–2.508(3) Å and d(Li3–S) = 2.413(4)–2.579(3) Å in Li_3AsS_3, respectively. The [$Li2S_4$] and [$Li3S_4$] tetrahedra are connected by sharing one corner. In contrast Li1 has a distorted square-pyramidal coordination by sulfur in the case of Li_3SbS_3 (d(Li1–S) = 2.52–2.78 Å) and an even more distorted square pyramidal surrounding in case of Li_3AsS_3. In fact, 5+1 coordination is found in both cases with the sixth sulfur atom in a distance of ca. 3.5 Å (Li_3SbS_3) and ca. 3.7 Å (Li_3AsS_3). Similar to Cu_3SbS_3 [14,15] and Cu_3SbSe_3[18] the structure of Li_3PnS_3 can be derived from the cementite type structure (Fe_3C).[26] In Fe_3C, there are trigonal prisms Fe_6 centered with carbon, and octahedral voids. In case of the title compounds iron is replaced by sulfur and carbon is replaced by the pnicogen atoms. However, the pnicogen atoms are located off center towards one triangular face of the prism. Thus, three short distances to sulfur are remaining

Special Issue

Table 3. Anisotropic displacement parameters U_{ij} for Li_3SbS_3 and Li_3AsS_3.

Li_3SbS_3						
Atom	U_{11}	U_{22}	U_{33}	U_{23}	U_{13}	U_{12}
Sb	0.017(1)	0.016(1)	0.015(1)	0.000(1)	–0.001(1)	0.001(1)
S1	0.022(1)	0.016(2)	0.015(1)	–0.002(1)	–0.001(1)	0.000(1)
S2	0.021(1)	0.016(1)	0.017(1)	–0.001(2)	0.001(2)	–0.002(1)
S3	0.024(1)	0.015(2)	0.019(2)	0.001(1)	–0.002(1)	–0.002(1)
Li1	0.025(7)	0.035(8)	0.05(1)	0.007(7)	0.001(6)	0.004(6)
Li2	0.024(6)	0.026(6)	0.019(7)	–0.001(5)	–0.008(5)	0.002(5)
Li3	0.040(8)	0.020(6)	0.036(9)	–0.013(6)	–0.001(6)	0.004(6)
Li_3AsS_3						
Atom	U_{11}	U_{22}	U_{33}	U_{23}	U_{13}	U_{12}
As	0.015(1)	0.016(1)	0.015(1)	0.000(1)	–0.001(1)	0.001(1)
S1	0.021(1)	0.016(1)	0.016(1)	–0.002(1)	0.000(1)	0.000(1)
S2	0.019(1)	0.015(1)	0.016(1)	0.001(1)	–0.002(1)	–0.002(1)
S3	0.023(1)	0.017(1)	0.015(1)	–0.001(1)	–0.001(1)	–0.001(1)
Li1	0.029(2)	0.024(2)	0.038(2)	0.003(1)	0.004(1)	–0.001(1)
Li2	0.027(1)	0.025(2)	0.027(1)	0.004(1)	0.001(1)	0.005(1)
Li3	0.031(2)	0.023(2)	0.032(2)	–0.002(1)	0.003(1)	0.001(1)

(see Figure 2). Lithium atoms are located in non-occupied sites of this cementite-like arrangement. However, the monovalent cations can be located in different positions in this structural arrangement. For the copper containing compounds four possibilities to arrange copper on the faces of the Q_6 octahedra are observed: on two opposite faces, on two faces sharing one corner or one edge, or on four faces.[27] In the lithium containing compounds Li2 and Li3 are located on two faces sharing one corner.

By contrast to the polymorphs of Cu_3SbS_3 Li1 is located within the S_6 octahedron (see Figure 3). However, it is shifted towards one corner of the surrounding octahedron. The distance to the sixth sulfur atom is d(Li1–S) = 3.518 Å (Li_3SbS_3) and d(Li1–S) = 3.694 Å (Li_3AsS_3), respectively. Thus, an effective coordination number of five results for Li1. Figure 4 shows the group-subgroup relationship of Li_3SbS_3 and Li_3AsS_3 with Fe_3C.

DFT Calculations

From DFT band structure calculations Li_3AsS_3 and Li_3SbS_3 are predicted as indirect semiconductors. To estimate the bandgap, electronic exchange and correlation were treated by pure DFT functionals (GGA) and additionally by increasingly applied hybrid functionals (see, for example references[32,33]). The first method tends to underestimate bandgaps of semiconductors (e.g. ΔE = 0.7 eV for Si), while the latter over estimates them. For the title compounds all applied functionals give the same band structure characteristics shown for the GGA result on Li_3SbS_3 (Figure 5). From the difference of valence band maximum (VBM) and conduction band minimum (CBM) a gap of 2.4 eV is calculated (Li_3AsS_3, GGA: 2.5 eV). A detailed analysis reveals that VBM and CBM are situated at different k points, namely Z and T. The predicted direct gap at Z is $\Delta E > 3.2$ eV. Applying the well-known hybrid functionals B3PW, B3LYP, and PBE0 (see literature[32] and references cited therein) the calculated gaps are 3.7 (3.9), 3.8 (4.0), and 4.0 (4.2) eV for Li_3SbS_3 (Li_3AsS_3), respectively. From these results one can conclude on optical gaps close to 3 eV for the title compounds, which are in line with the observation of colorless crystals. The electronic gaps are due to the splitting of Sb-5p (As-4p) states due to bonding to S-3p as provided from the atomic site projected density of states (DOS, Figure 6). The CBM is mainly formed by antibonding Sb-5p states with minor contributions of S-3p. Concerning the valence band (VB) three major contributions can be distinguished due to bonding states from Sb-5p to S-3p (–3 to –4 eV) and nonbonding S-3p. The top of the VB must be attributed to nonbonding Sb-5p states. Li-2s and 2p-orbitals contribute mainly to antibonding states above 5 eV.

Impedance Spectroscopy

Impedance spectroscopic measurements on cold pressed samples of Li_3SbS_3 were performed using gold as ion blocking electrode material. Nyquist plots show the typical behavior of an ionic conductor consisting of semicircles at high frequencies and diffusion arcs at low frequencies. Selected ionic conductivities are $1.6 \times 10^{-9}\ \Omega^{-1}\,cm^{-1}$ at 323 K and $5.4 \times 10^{-5}\ \Omega^{-1}\,cm^{-1}$ at 573 K. The corresponding Arrhenius diagram provides an activation energy of 0.72 eV. Temperature dependent ionic conductivities of Li_3SbS_3 are shown in Figure 7. Comparable results have been already provided on this compound.[39] Ionic transport measurements gave an E_A of 0.40 eV and the absorption edge was determined to 3.55 eV. This corresponds well to our results from impedance measurements (E_A = 0.72 eV) and DFT calculations (optical gaps close to 3 eV).

Raman Spectroscopy

Raman measurements were performed on Li_3SbS_3 samples in sealed Duran glass capillaries. The spectra are dominated by strong stretching bands of the $[SbS_3]^{3-}$ units. The Sb–S

Zeitschrift für anorganische und allgemeine Chemie ZAAC Journal of Inorganic and General Chemistry

Table 4. Selected interatomic distances /Å and angles /° for Li_3SbS_3 and Li_3AsS_3 at room temperature.

Li_3SbS_3				
Sb1–S1		2.423(4)	S1–Sb1–S3	102.55(6)
Sb1–S2		2.446(1)	S1–Sb1–S2	98.6(1)
Sb1–S3		2.434(4)	S3–Sb1–S2	97.0(1)
Li1–S1	2×	2.52(1)	S1–Li1–S1	106.6(5)
Li1–S2		2.74(2)	S1–Li1–S3	158.2(6)
Li1–S2		2.78(2)	S1–Li1–S3	94.6(4)
Li1–S3		2.63(1)	S1–Li1–S2	89.1(4)
			S1–Li1–S2	106.1(5)
			S3–Li1–S2	89.7(4)
			S1–Li1–S2	87.8(4)
			S1–Li1–S2	96.3(5)
			S3–Li1–S2	85.1(4)
			S2–Li1–S2	157.4(5)
Li2–S1		2.47(1)	S2–Li2–S3	108.4(5)
Li2–S2		2.41(1)	S2–Li2–S1	127.3(5)
Li2–S3		2.44(1)	S3–Li2–S1	100.9(4)
Li2–S3		2.49(1)	S2–Li2–S3	100.7(4)
			S3–Li2–S3	109.7(5)
			S1–Li2–S3	109.2(5)
Li3–S1		2.51(2)	S3–Li3–S1	103.8(5)
Li3–S2		2.52(1)	S3–Li3–S2	127.4(6)
Li3–S2		2.60(1)	S1–Li3–S2	103.5(5)
Li3–S3		2.42(1)	S3–Li3–S2	110.0(5)
			S1–Li3–S2	92.1(4)
			S2–Li3–S2	113.0(5)
Li_3AsS_3				
As1–S1		2.252(1)	S3–As1–S2	100.38(2)
As1–S2		2.260(1)	S3–As1–S1	103.84(2)
As1–S3		2.275(1)	S2–As1–S1	101.99(2)
Li1–S1		2.478(3)	S1–Li1–S1	110.3(1)
Li1–S1		2.495(3)	S1–Li1–S3	153.5(2)
Li1–S2		2.731(4)	S1–Li1–S3	95.6(1)
Li1–S2		2.754(4)	S1–Li1–S2	84.8(1)
Li1–S3		2.576(4)	S1–Li1–S2	109.8(1)
			S3–Li1–S2	91.7(1)
			S1–Li1–S2	89.3(1)
			S1–Li1–S2	97.8(1)
			S3–Li1–S2	81.6(1)
			S2–Li1–S2	152.1(1)
Li2–S1		2.462(4)	S2–Li2–S3	106.3(1)
Li2–S2		2.439(3)	S2–Li2–S1	122.8(1)
Li2–S3		2.449(3)	S3–Li2–S1	99.8(1)
Li2–S3		2.508(3)	S2–Li2–S3	100.7(1)
			S3–Li2–S3	110.2(1)
			S1–Li2–S3	116.6(1)
Li3–S1		2.530(4)	S3–Li3–S1	103.4(2)
Li3–S2		2.539(4)	S3–Li3–S2	124.5(1)
Li3–S2		2.579(3)	S1–Li3–S2	102.7(1)
Li3–S3		2.413(4)	S3–Li3–S2	112.5(1)
			S1–Li3–S2	92.2(1)
			S2–Li3–S2	114.4(2)

stretching modes for these units are located between 330 and 360 cm^{-1}.[21,24,40–42] For Li_3SbS_3, the $[SbS_3]^{3-}$ units are isolated but surrounded by five additional sulfur atoms in the range of so called secondary bonds (d(Sb–S) = 3.72–3.89 Å).

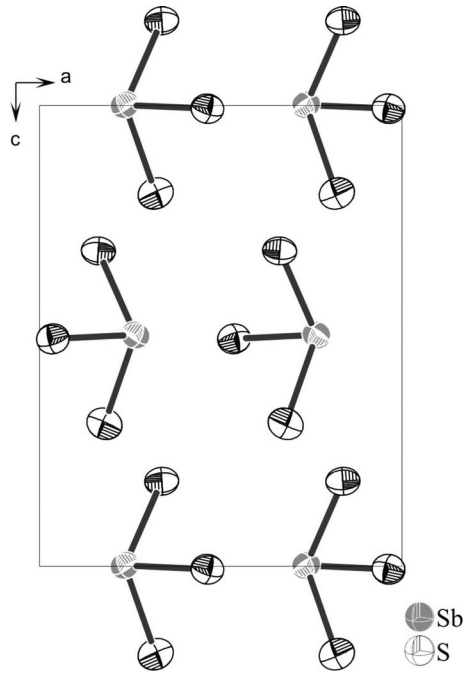

Figure 1. Arrangement of the $[SbS_3]^{3-}$ units along the b axis. Lithium ions are omitted for clarity.

Due to additional Sb–S bonds, the bands are red-shifted.[21,40] For the title compound, the vibrations are observed at 333, 317, and 301 cm^{-1}. The Raman spectrum is shown in Figure 8. Compared to the Raman spectra of Cu_3SbS_3,[21] $(CuI)_2$-Cu_3SbS_3,[21] and $(AgI)_2Ag_3SbS_3$,[24] lowering the symmetry of the $[SbS_3]^{3-}$ unit from C_s to C_1 leads to a splitting of the modes.

Conclusions

Li_3SbS_3 is structurally characterized as a new member of the $M^I{}_3PnQ_3$ chalcogenometalate family. It crystallizes orthorhombically in the space group $Pna2_1$ (no. 33). Li_3SbS_3 is isotypic to Li_3AsS_3, which was prepared by a new synthesis route. Herein, LiI serves as a flux and is not incorporated in the structure of Li_3AsS_3. Li_3AsS_3 crystallizes as colorless rods and not as green crystals as published earlier.[3] This fits with results from electronic structure calculations that predict bandgaps of approximately 3 eV for both compounds. The gaps are determined by splitting of bonding and antibonding states from bonding of Sb-5p (As-4p) to S-3p. Impedance spectroscopic measurements show high ionic conductivity for Li_3SbS_3. The conductivity is in the range of 1.6×10^{-9} Ω^{-1} cm^{-1} at 323 K and 5.4×10^{-5} Ω^{-1} cm^{-1} at 573 K. The corresponding Arrhenius plot provides an activation energy of 0.72 eV. Raman spectra of Li_3SbS_3 are dominated by strong stretching modes of the $[SbS_3]^{3-}$ units at 333, 317, and 301 cm^{-1}, which indicates a strong influence of the sulfur atoms in a so-called non-bonding distance to antimony.

Experimental Section

Synthesis: Li_3SbS_3 was prepared by reaction of Li_2S (99.9 %, Alfa Aesar) and Sb_2S_3 (Merck) in the ratio 3:1, Li_3AsS_3 of LiI (anhydrous,

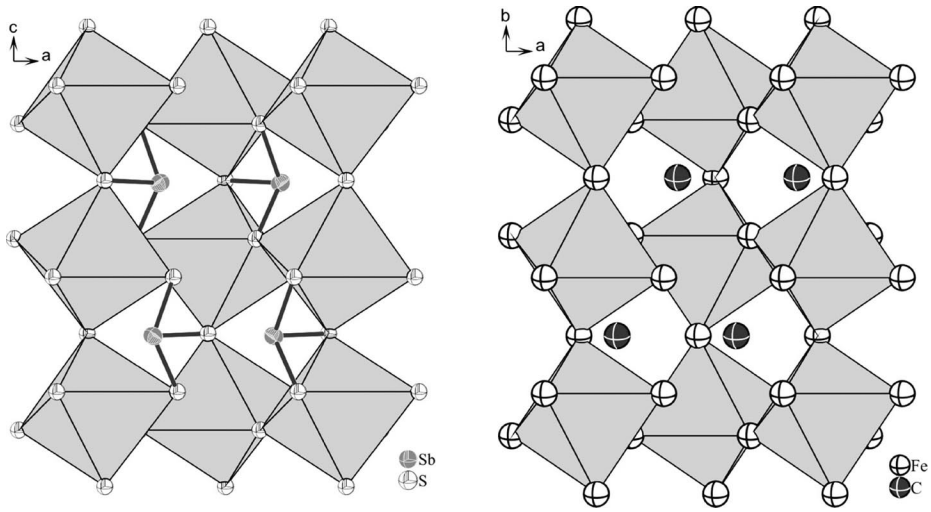

Figure 2. Section of the crystal structures of Li_3SbS_3 and Fe_3C showing the structural similarities between both compounds. Lithium ions are omitted for clarity.

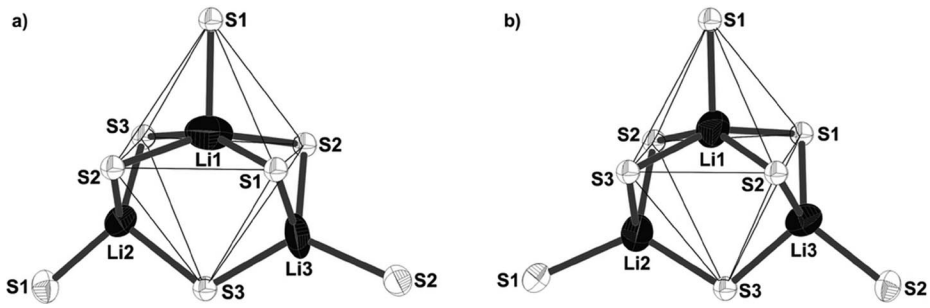

Figure 3. Occupation of the S_6-octahedra in Li_3SbS_3 (a) and Li_3AsS_3 (b). Li2 and Li3 are located on two faces sharing one corner. Both are coordinated by four sulfur atoms in a distorted tetrahedral manner. Li1 is located in the S_6-octahedron, but significantly shifted to one corner. Thus, it is regarded as only five-coordinate.

Merck), Li (99.999 %, Merck), As (99.999 %, Alfa Aesar), and S (99.9995 %, Merck) in the ratio 2:3:1:3. All preparations were performed in a glove box in an atmosphere of argon. The reagents were filled in graphitized, evacuated silica ampoules. For Li_3SbS_3, the starting materials were annealed for 3 weeks at 500 °C, for Li_3AsS_3, the materials were slowly heated up to 200 °C, then faster to 450 °C, and were further annealed for 1 week at 350 °C. Pale grey crystals of Li_3SbS_3 and colorless crystals of Li_3AsS_3, suitable for single-crystal X-ray structure determination, could be separated from the reaction product. Both products are air and moisture sensitive.

X-ray Crystallography: For the structure determination at room temperature single crystals were filled in a closed glass capillary and mounted on an Oxford Diffraction Gemini R Ultra CCD providing monochromatic Mo-K_α radiation (λ = 0.71073 Å) in the case of Li_3SbS_3. Absorption was corrected by multi-scans.[29] For Li_3AsS_3 the crystals were mounted on an IPDS (Stoe) single crystal diffractometer providing monochromatic Mo-K_α radiation (λ = 0.71073 Å). Absorption was corrected numerically after an optimization of the description of the crystal shape with the X-SHAPE routine.[31] Crystallographic data are collected in Table 1. The crystal structures were solved by Direct Methods (SIR92).[36] Li positions were located from difference Fourier maps. All atoms were refined by using anisotropic displacement parameters. An extinction parameter was included in the last refinement stages for Li_3AsS_3, in case of Li_3SbS_3 it was equal to zero within the e.s.d. and therefore not refined. The *z*-coordinate of Sb and As, respectively, were fixed during the refinement in order to make the positional parameters as comparable as possible. The Flack-parameter is equal to zero in both cases, indicating that no inversion twinning is observed.

DFT Methods: The electronic structures were calculated with the codes CRYSTAL09[33] and FPLO9.[34] The first one additionally allows for the use of GGA (PBE[35]) and hybrid functionals (B3PW, B3LYP, PBE0, see references[32,33]). The band structure calculation results were confirmed from all electron and valence basis sets, as well as from PBE calculations with the full-potential local orbital-code FPLO9.[34] For this code extended all electron basis sets are optimized at each cycle of the SCF routine. The k-points mesh was converged to $12 \times 12 \times 12$ shrinking factors.

Impedance Spectroscopy: Impedance spectroscopic investigations were performed in the frequency range 1 Hz to 1 MHz and the temperature range 323 K to 573 K (IM6d, Zahner Elektrik). The powdered samples of Li_3SbS_3 were cold pressed into pellets with 6000 kg·cm^{-2}, resulting in a density of > 90 % of the calculated density. They were contacted in a spring loaded cell between gold electrodes. Details of the experimental setup are given elsewhere.[37]

Raman Spectroscopy: Raman measurements were carried out with a Varian Fourier transform Raman module coupled to a Varian FTS 7000e spectrometer equipped with a Nd:YAG laser (excitation wave-

Zeitschrift für anorganische und allgemeine Chemie ZAAC Journal of Inorganic and General Chemistry

Pnma **Fe_3C**			t2 *a*, *c*, *-b* +(0, 0, 1/4)	***Pna*2$_1$** **Li_3AsS_3** **Li_3SbS_3**	
Pnma *a*, *b*, *c* **Fe_3C**	→	***Pnam*** *a*, *c*, *-b* **Fe_3C**	→ ***Pna*2$_1$** +(0,0,1/4)	→ ***Pna*2$_1$** **Li_3AsS_3**	***Pna*2$_1$** **Li_3SbS_3***
				4*a*: S1	**4*a*: S1**
			4*a*:	**1**	**1**
			1	0.1607	0.1633
			0.1815	0.2909	0.3034
8*d*: Fe1		**8*d*: Fe1**	0.3375	0.1733	0.1826
1		**1**	0.1834		
0.1815		0.1815			
0.0666		0.3375	**4*a*:**	**4*a*: S3**	**4*a*: S3**
0.3375		0.9334	**1**	**1**	**1**
			0.8185	0.8153	0.8212
			0.6625	0.7197	0.7039
			0.3166	0.3139	0.3073
4*c*: Fe2		**4*c*: Fe2**	**4*a*:**	**4*a*: S2**	**4*a*: S2**
.m.		**.m.**	**1**	**1**	**1**
0.0367		0.0367	0.0367	0.0445	0.0367
1/4		0.8402	0.8402	0.8601	0.8637
0.8402		3/4	0	0.9902	0.9919
4*c*: C		**4*c*: C**	**4*a*:**	**4*a*: As1**	**4*a*: Sb1**
.m.		**.m.**	**1**	**1**	**1**
0.8770		0.8770	0.8770	0.7467	0.7646
1/4		0.4440	0.4440	0.4028	0.3951
0.4440		3/4	0	0	0

Figure 4. Symmetry relations between Li_3SbS_3 / Li_3AsS_3 and Fe_3C (Bärnighausen-Stammbaum).[28] Upon the transition from *Pnam* to *Pna*2$_1$ the 8*d* site splits into two 4*a* sites. *Structural data for Li_3SbS_3 are inverted for comparison.

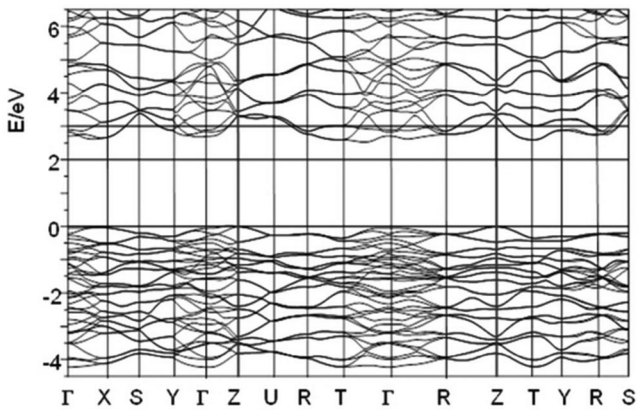

Figure 5. Electronic band structure (GGA), lines are pointed out as guide for the eyes at $k = Z$ and $E = 3$ eV.

length $\lambda = 1064$ nm) and a liquid nitrogen cooled germanium detector. The powdered samples of Li_3SbS_3 were sealed in Duran glass capillaries. The resolution was 2 cm^{-1} and the spectrum was processed with the Varian Resolutions Pro software.[38]

Further details of the crystal structure investigations may be obtained from the Fachinformationszentrum Karlsruhe, 76344 Eggenstein-Leopoldshafen, Germany (Fax: +49-7247-808-666; E-Mail: crysdata@fiz-karlsruhe.de, http://www.fiz-karlsruhe.de/request for deposited data.html) on quoting the depository numbers CSD-424834 (Li_3SbS_3) and CSD-424835 (Li_3AsS_3).

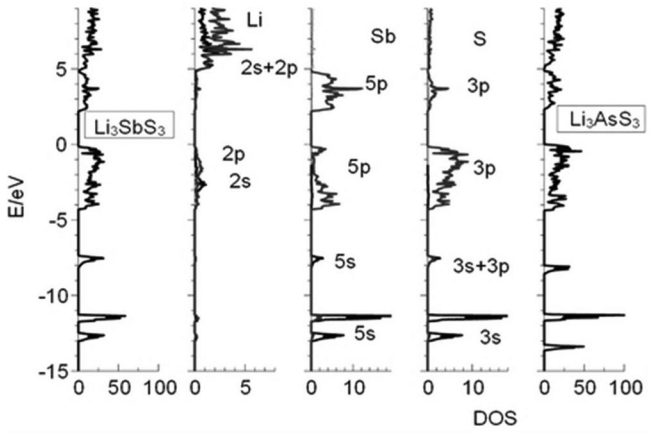

Figure 6. Electronic density of states and atomic site projections for Li_3SbS_3, and total DOS for Li_3AsS_3.

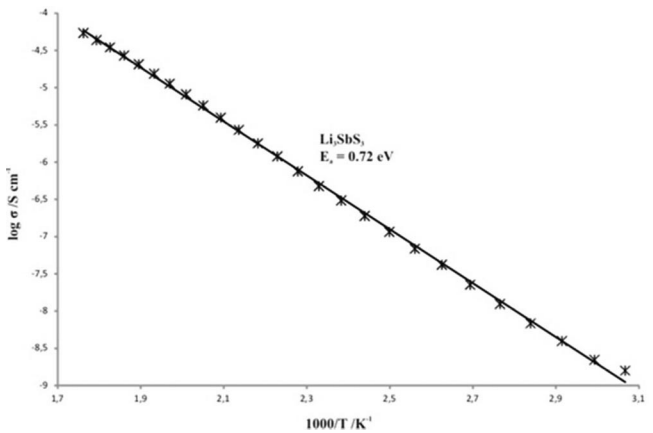

Figure 7. Temperature dependence of the ionic conductivity of Li_3SbS_3.

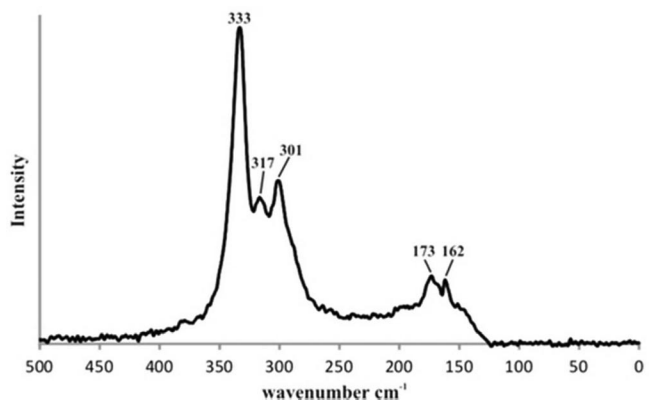

Figure 8. Raman spectrum of Li_3SbS_3. It is dominated by the stretching modes of the $[SbS_3]^{3-}$ units.

Acknowledgements

We thank *Dr. M. Bodensteiner* for collecting single-crystal X-ray diffraction data of Li_3SbS_3.

References

[1] H. Sommer, R. Hoppe, *Z. Anorg. Allg. Chem.* **1977**, *430*, 199.
[2] W. Bronger, A. Donike, D. Schmitz, *Z. Anorg. Allg. Chem.* **1999**, *625*, 435.
[3] D.-Y. Seung, P. Gravereau, L. Trut, A. Levasseur, *Acta Crystallogr. Sect. C* **1998**, *54*, 900.
[4] C. Preitschaft, *Dissertation*, Regensburg **2004**.
[5] M. Palazzi, *Acta Crystallogr., Sect. B* **1976**, *32*, 3175.
[6] W. Bronger, A. Donike, D. Schmitz, *Z. Anorg. Allg. Chem.* **1998**, *624*, 553.
[7] W. Bronger, A. Donike, D. Schmitz, *Z. Anorg. Allg. Chem.* **1996**, *622*, 1003.
[8] W. Bronger, A. Donike, D. Schmitz, *Z. Anorg. Allg. Chem.* **1997**, *623*, 1715.
[9] D. Harker, *J. Chem. Phys.* **1936**, *4*, 381.
[10] P. Engel, W. Nowacki, *Acta Crystallogr., Sect. B* **1968**, *24*, 77.
[11] K. Sakai, T. Koide, T. Matsumoto, *Acta Crystallogr., Sect. B* **1978**, *34*, 3326.
[12] K. Kihara, T. Matsumoto, *Z. Kristallogr.* **1986**, *177*, 211.
[13] M. G. Kanatzidis, J.-H. Chou, *J. Solid State Chem.* **1996**, *127*, 186.
[14] A. Pfitzner, *Z. Anorg. Allg. Chem.* **1994**, *620*, 1992.
[15] A. Pfitzner, *Z. Kristallogr.* **1998**, *213*, 228.
[16] S. Karup-Møller, E. Makovicky, *Am. Mineral.* **1974**, *59*, 889.
[17] B. J. Skinner, F. D. Luce, E. Makovicky, *Econ. Geol.* **1972**, *67*, 924.
[18] A. Pfitzner, *Z. Anorg. Allg. Chem.* **1995**, *621*, 685.
[19] E. J. Skoug, J. D. Cain, D. T. Morelli, *Appl. Phys. Lett.* **2010**, *96*, 181905.
[20] M. Kirkham, P. Majsztrik, E. Skoug, D. Morelli, H. Wang, W. D. Porter, E. A. Payzant, E. Lara-Curzio, *J. Mater. Res.* **2011**, *26*, 2001.
[21] A. Pfitzner, *Chem. Eur. J.* **1997**, *3*, 2032.
[22] T. J. Bastow, H. J. Whitfield, *J. Solid State Chem.* **1981**, *40*, 203.
[23] T. Nilges, *Dissertation*, Siegen **2000**.
[24] T. Nilges, S. Reiser, J. H. Hong, E. Gaudin, A. Pfitzner, *Phys. Chem. Chem. Phys.* **2002**, *4*, 5888.
[25] A. Pfitzner, C. Preitschaft, F. Rau, *Z. Anorg. Allg. Chem.* **2004**, *630*, 75.
[26] E. J. Fasiska, G. A. Jeffrey, *Acta Crystallogr.* **1965**, *19*, 463.
[27] A. Pfitzner, *Habilitationsschrift*, Siegen **2000**.
[28] H. Bärnighausen, *MATCH* **1980**, *9*, 139.
[29] SCALE3 ABSPACK, *CrysAlis RED* software, Version 171.35.21; Oxford Diffraction Ltd: Oxford, UK, **2006**.
[30] G. M. Sheldrick, *SHELX 97* Programs for Solution and Refinement of Crystal Structures, University of Göttingen, Germany, **1997**.
[31] *X-SHAPE*, STOE, Darmstadt, Germany, **1996**.
[32] a) X. Zheng, A. J. Cohen, P. Mori-Sánchez, X. Hu, W. Yang, *Phys. Rev. Lett.* **2011**, *107*, 0264031; b) S. Tomic, B. Montanari, N. M. Harrison, *Phys. E* **2008**, *40*, 2125.
[33] R. Dovesi, V. R. Saunders, C. Roetti, R. Orlando, C. M. Zicovich-Wilson, F. Pascale, B. Civalleri, K. Doll, N. M. Harrison, I. J. Bush, P. D'Arco, M. Llunell, CRYSTAL09, User's Manual. University of Torino, Torino, **2009**.
[34] K. Köpernik, H. Eschrig, *Phys. Rev. B* **1999**, *59*, 1743.
[35] J. P. Perdew, K. Burke, M. Ernzerhof, *Phys. Rev. Lett.* **1996**, *77*, 3865.
[36] A. Altomare, G. Cascarano, C. Giacovazzo, A. Guagliardi, *J. Appl. Crystallogr.* **1993**, *26*, 343.
[37] E. Freudenthaler, A. Pfitzner, *Solid State Ionics* **1997**, *101–103*, 1053.
[38] *Resolutions Pro Software*, Molecular Spectroscopy Solutions, Varian Inc., Version 4.1.0.101, **2006**.
[39] J. Olivier-Fourcade, M. Maurin, E. Philippot, *Solid State Ionics* **1983**, *9,10*, 135.
[40] A. Pfitzner, D. Kurowski, *Z. Kristallogr.* **2000**, *215*, 373.
[41] V. Spetzler, C. Näther, W. Bensch, *Inorg. Chem.* **2005**, *44*, 5805.
[42] R. Kiebach, R. Warratz, C. Näther, W. Bensch, *Z. Anorg. Allg. Chem.* **2009**, *635*, 988.

Received: June 14, 2012
Published Online: September 7, 2012

